Manufacturing Letters 35 (2023) 48–52

Contents lists available at ScienceDirect

Manufacturing Letters

journal homepage: www.elsevier.com/locate/mfglet

Repairing surface defects of Zr-based metallic glass ribbons by nanosecond pulsed laser irradiation

Jingtao Wang [a], Hongyang Zhang [a], Zhiyu Zhang [b], Jing Hong [a], Yongfeng Qian [a], Hu Huang [a,*], Jiwang Yan [c]

[a] Key Laboratory of CNC Equipment Reliability, Ministry of Education, School of Mechanical and Aerospace Engineering, Jilin University, Changchun, Jilin 130022, China
[b] Key Laboratory of Optical System Advanced Manufacturing Technology, Changchun Institute of Optics, Fine Mechanics and Physics, Chinese Academy of Sciences, Changchun, China
[c] Department of Mechanical Engineering, Faculty of Science and Technology, Keio University, Yokohama 223-8522, Japan

ARTICLE INFO

Article history:
Received 5 September 2022
Received in revised form 15 November 2022
Accepted 25 November 2022
Available online 20 December 2022

Keywords:
Amorphous materials
Laser processing
Metallic glass ribbon
Surface defects
Nanosecond pulsed laser

ABSTRACT

The metallic glass ribbons (MGRs) industrially produced by the single roller melt-spun method have many surface defects such as pits and scratches. In this study, it was attempted to repair the surface defects of Zr-based MGRs via nanosecond pulsed laser irradiation. The experimental results showed that the roughness of laser-repaired surfaces was significantly reduced compared to the melt-spun surface, and the surface topographies and morphologies were sensitive to the laser parameters. With optimal laser parameters, the smooth and defect-free surface could be achieved. This work offers a convenient and high-efficiency approach for repairing the surface defects of MGRs.

1. Introduction

With some unique characteristics such as high strength, high corrosion resistance, and excellent wear resistance [1,2], metallic glass ribbons (MGRs) are very promising structural and functional materials. For MGRs, previous studies mainly focused on solving their size [3,4] and surface oxidation problems [5], and the surface quality issues are generally ignored. Specifically, the MGRs surfaces suffer from various defects, such as pits and scratches which severely limit their engineering applications. The conventional methods such as chemical mechanical polishing [6] and electrochemical polishing [7], may be not applicable for repairing the surface defects due to the flexibility and thin structure of MGRs. While, laser processing on the other hand has been widely used to fabricate micro/nano structures on bulk metallic glasses [8–11], as well as modify their surface mechanical properties [12–15]. For example, Qian et al. [9] used a nanosecond pulsed laser to fabricate micro-convex array structures on a Zr-based MG surface which tuned the light reflection characteristic. By laser nitriding, surface hardness of the Zr-based MG was significantly increased by Hong et al. [12]. With features of non-contact processing and high heating/cooling rates, nanosecond pulsed laser irradiation was attempted here to repair the surface defects of MGRs and improve their surface quality. By optimizing the irradiation parameters, defect-free smooth surfaces were successfully achieved. The roughness and three-dimensional topographies of the laser-repaired surfaces were characterized, and the surface morphology evolution was analyzed. This work offers a convenient and high-efficiency approach for repairing the surface defects of MGRs.

2. Materials and experiments

The Zr-based MGRs with nominal compositions of $Zr_{41.2}Ti_{13.8}Cu_{12.5}Ni_{10}Be_{22.5}$ were prepared by single roller melt-spinning under vacuum. All ribbons with a cross section of about 0.05 mm × 4 mm were cut into slices with the length of 20 mm. Before laser processing, the amorphous feature of the ribbons was confirmed by X-ray diffraction (XRD, D8 Advance, Bruker, Germany). Then, the samples were placed in an atmosphere chamber with flowing argon, and the pressure was maintained at 0.01 MPa. A nanosecond pulsed laser (SP-050P-A-EP-Z-F-Y, SPI Lasers, UK) with a wavelength of 1064 nm was used for irradiation experiments. The laser beam diameter was about 43 μm with a Gaussian energy distribution. The pulse width and repetition frequency were 20 ns and 353 kHz, respectively. Generally, the peak laser power intensity (I), overlap rate (r), number of irradiation cycles (N) and scanning speed (v) would greatly affect the surface quality. Therefore, these four parameters were investigated by orthogonal experiments, and

* Corresponding author.
E-mail address: huanghu@jlu.edu.cn (H. Huang).

https://doi.org/10.1016/j.mfglet.2022.11.008

an optimal set of parameters was obtained, i.e., I = 3.85 × 10^9 W/m^2, r = 88.4 %, N = 6 and v = 900 mm/s. For the purpose of investigating the influence of each parameter on laser repairing, 20 cases of experiments were designed according to the optimal parameters, as listed in Table 1. The other parameters were kept constant when one parameter was varied.

Table 1
Experimental parameters for laser repairing.

Case	I (×10^9 W/m^2)	r (%)	N	v (mm/s)
1	3.51	88.4	6	900
2	3.66	88.4	6	900
3	3.85	88.4	6	900
4	3.96	88.4	6	900
5	3.99	88.4	6	900
6	3.85	30.2	6	900
7	3.85	53.5	6	900
8	3.85	76.7	6	900
9	3.85	88.4	6	900
10	3.85	93.4	6	900
11	3.85	88.4	4	900
12	3.85	88.4	5	900
13	3.85	88.4	6	900
14	3.85	88.4	7	900
15	3.85	88.4	8	900
16	3.85	88.4	6	700
17	3.85	88.4	6	800
18	3.85	88.4	6	900
19	3.85	88.4	6	1000
20	3.85	88.4	6	1100

After laser irradiation, the roughness and three-dimensional (3D) topographies of the irradiated areas were measured by the laser confocal scanning microscope (LCSM, OLS4100, Olympus, Japan). The measurement area was 256 μm × 256 μm, and the roughness values of five measurements were averaged. Furthermore, a tungsten filament scanning electron microscope (SEM, JSM-IT500A, JEOL, Japan) was used to characterize the morphology evolution of the laser-irradiated surfaces.

3. Results and discussion

Fig. 1(a)-(d) present the surface roughness (Sa) of the melt-spun surface and laser irradiated surfaces obtained under various I, r, N and v, respectively. As shown in Fig. 1(a), the melt-spun surface possesses a large Sa (namely, 419.6 nm), while the surface roughness of laser repaired surfaces decreases significantly. When the I increases, the Sa decreases first and then increases again, and the minimum Sa (namely, 61.8 nm) is obtained at 3.85 × 10^9 W/m^2. In Fig. 1(b), the Sa decreases slowly and reaches a minimum value when the r is 88.4 %. However, when further increasing the r to 93.4 %, the change of Sa is very slight, demonstrating that the larger r has little significant effect on the surface roughness. Fig. 1(c) shows the change of Sa under different N, which is similar to the trend in Fig. 1(a). In addition, the Sa shows a negligible change when v increases from 700 to 1100 mm/s in Fig. 1(d), suggesting that the employed scanning speed has almost no effect on the roughness of the irradiated surfaces. From the above analysis, it is seen that the Zr-based MGRs can be repaired by nanosecond pulsed laser irradiation, and the best surface quality with Sa of

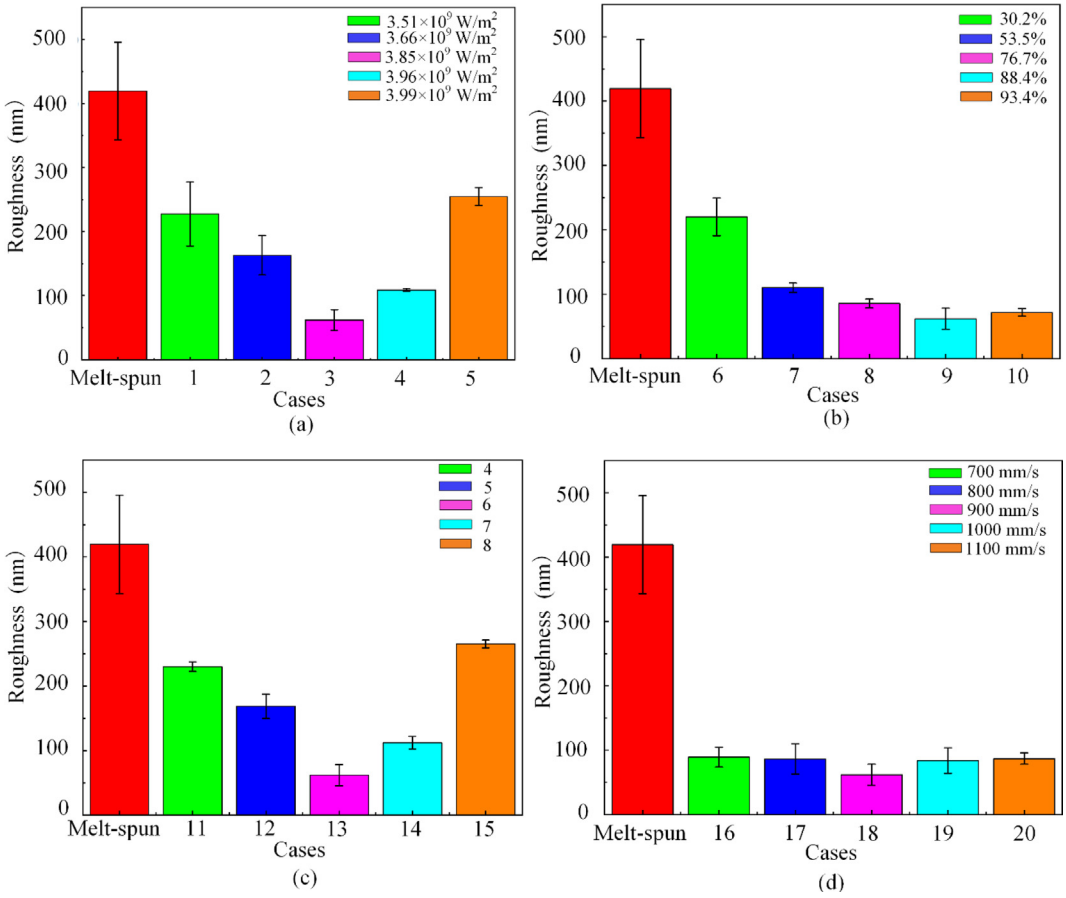

Fig. 1. Sa of the melt-spun and laser repaired surfaces obtained under various (a) peak laser power intensities, (b) overlap rates, (c) numbers of irradiation cycles, and (d) scanning speeds.

61.8 nm can be achieved under the optimal parameters according to the orthogonal design. In addition, it can be concluded that for the used parameter ranges, the peak laser power intensity, overlap rate and number of irradiation cycles have significant effects on the surface roughness, while the effect of the scanning speed is relatively slight.

To study the change in 3D topography, the melt-spun surface and representative laser-repaired surfaces are observed by using the LCSM, and the results are shown in Fig. 2. Fig. 2(a) and (b) indicate that after laser repairing, the peak-valley height of the surface decreases from 14 μm to 6 μm. Moreover, from Fig. 2(c), it is seen that the height of the repaired surface has less drastic fluctuation than that of the melt-spun. This can be attributed to the molten role of laser, and the molten material fills into the surface defects [16]. From Fig. 2(d), (b) and (g), it is noted that the peak-valley height of the repaired surfaces decreases first and then increases again when the I increases. Excessive molten material in the center of the pool flows to the edges when a relatively high I is applied [17,18], resulting in a larger surface height. As shown in Fig. 2(e), (b) and (h), the larger r leads to over melting, which in turn aggravates the re-solidification of the uneven surface [19][11], making the surface height increase. Increasing the N prolongs the interaction time between the laser and material and affects the degree of melting [20], but the redundant irradiation time would enhance the fluidity of the melt and cause an increase in surface height, as shown in Fig. 2(f), (b) and (i).

Fig. 3 presents the SEM morphologies of the Zr-based MGRs surfaces before and after laser repairing. For the melt-spun surface as shown in Fig. 3(a), the presence of many pits and scratches results in the high roughness and peak-valley height. Fig. 3(b) shows the SEM morphology of the laser repaired surface (case 3). No obvious pits and scratches can be observed, indicating that the defects on the original surface have been repaired. From Fig. 3(c) and (f), when the I is low, the surface defects are partly repaired due to inadequately melting of the material, and with the I increasing, the surface heat accumulates severely [17,21], causing the surface material to rapidly melt, evaporate and generate the ejection phenomenon, which eventually leads to an uneven ablated surface. In Fig. 3(d) and (g), it is evident that when the r increases, the surfaces become smooth gradually. As for Fig. 3(e) and (h), although the repetitive laser repairing greatly improves the surface quality, significant height difference appears on the repaired surfaces. This could be mainly due to the increasingly intense flow of the melt under surface tension and gravity, as well as the increasing depth of the molten layer [22,23].

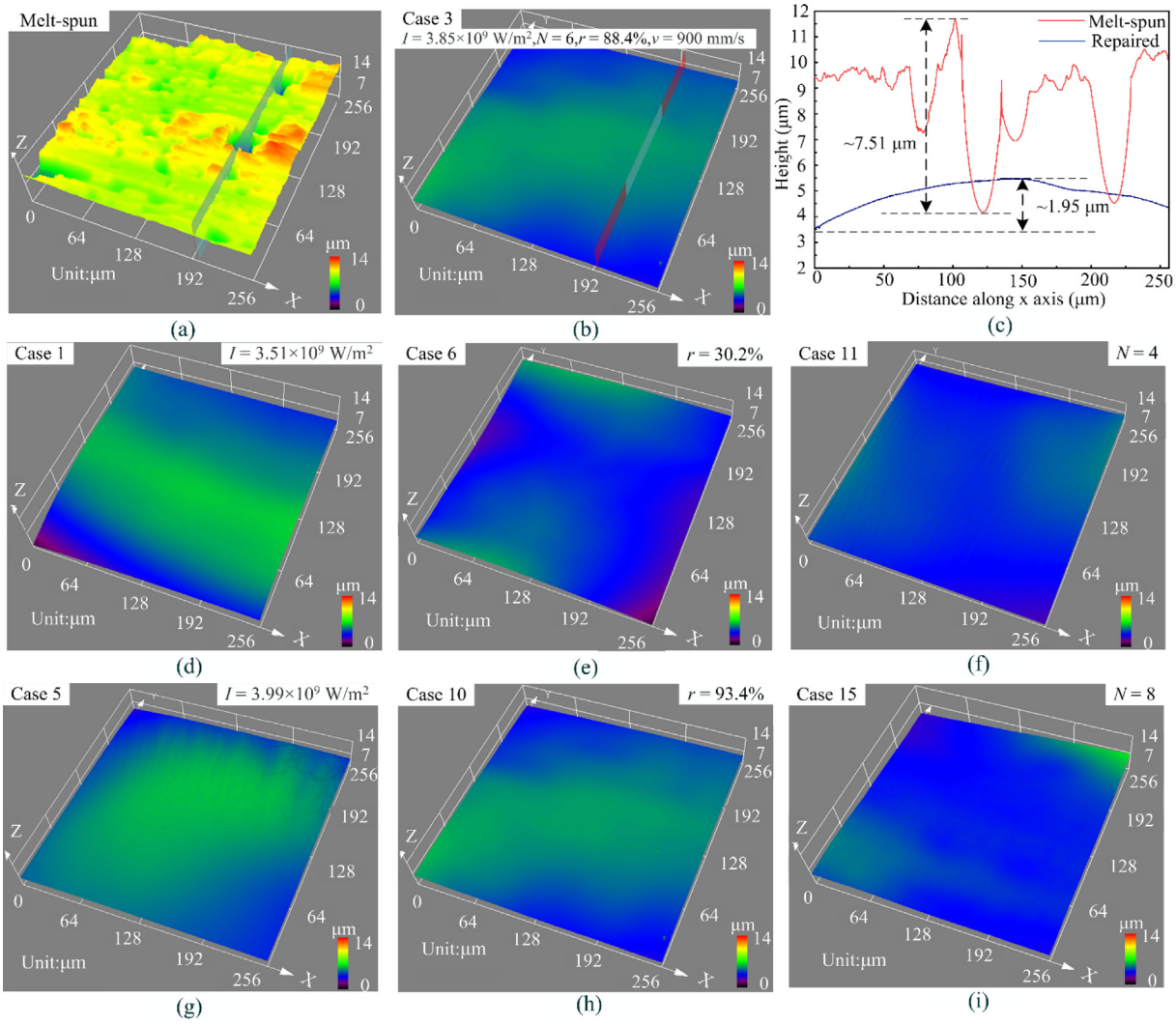

Fig. 2. 3D topographies of (a) melt-spun, (b) case 3, (d) case 1, (e) case 6, (f) case 11, (g) case 5, (h) case 10 and (i) case 15 surfaces. (c) shows the height of melt-spun and laser repaired surface (case 3).

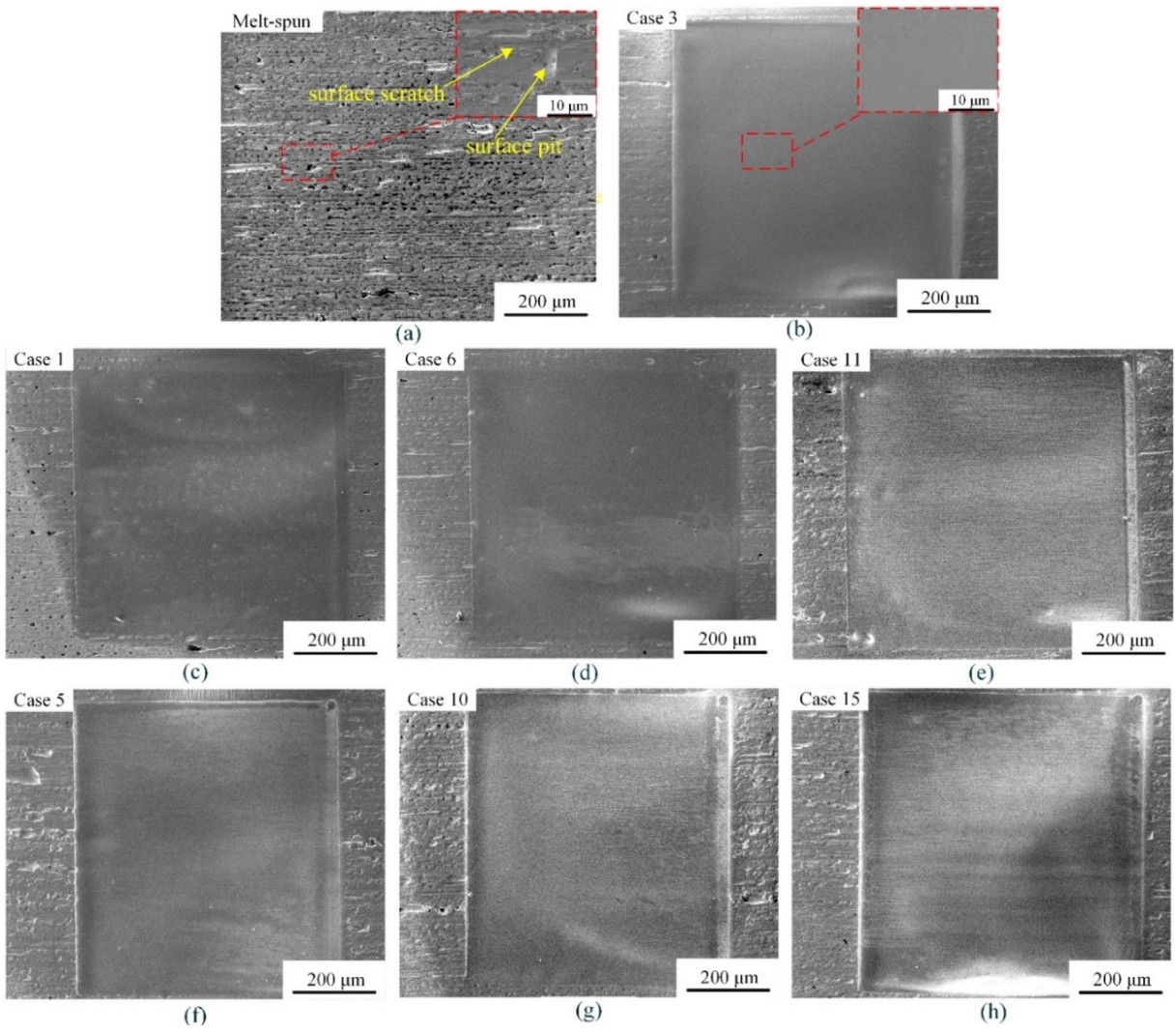

Fig. 3. SEM morphologies of (a) melt-spun, (b) case 3, (c) case 1, (d) case 6, (e) case 11, (f) case 5, (g) case 10, and (h) case 15 surfaces.

4. Conclusion

In summary, surface defects of Zr-based MGRs were successfully repaired via nanosecond laser irradiation in argon atmosphere. The influence of laser irradiation parameters on the 3D topographies and surface morphology evolution of the laser repaired areas was explored. Under optimal experimental conditions, the surface pits and scratches could be completely removed, and the surface roughness was decreased from 419.6 nm to 61.8 nm. The current finding offers a convenient and high-efficiency approach for repairing the surface defects of MGRs.

Declaration of Competing Interest

The authors declare that they have no known competing financial interests or personal relationships that could have appeared to influence the work reported in this paper.

Acknowledgements

This work was supported by the Natural Science Foundation of Jilin Province (20220101198JC) and the National Natural Science Foundation of China (Grant No. 51705197).

References

[1] Liu Y, Wang G, Wang R, Zhao D, Pan M, Wang W. Super plastic bulk metallic glasses at room temperature. Sci 2007;315(5817):1385–8.
[2] Liao C, Liu M, Zhang Qi, Dong W, Zhao R, Li B, et al. Low-temperature thermoplastic welding of metallic glass ribbons for in-space manufacturing面向太空制造的非晶合金条带的低温热塑性焊接. Sci China Mater 2021;64(4):979–86.
[3] Li JF, Sun YH, Ding DW, Wang WH, Bai HY. Nanosecond-pulsed laser welding of metallic glass. J Non-Crystal Solids 2020;537:120016.
[4] Chen B, Shi T, Li M, Yang F, Yan F, Liao G. Laser welding of annealed $Zr_{55}Cu_{30}Ni_5Al_{10}$ bulk metallic glass. Inter 2014;46:111–7.
[5] Zhang Q, Hui X, Li Z, Zhang G, Lin J, Li X, et al. Effect of pre-oxidation treatment on corrosion resistance of FeCoSiBPC. Amorph Alloy Mater 2022;15:3206.
[6] Zhao D, Lu X. Chemical mechanical polishing: Theory and experiment. Fric 2013;1(4):306–26.
[7] Simka W, Mosiałek M, Nawrat G, Nawrat G, Nowak P, Żak J, et al. Electrochemical polishing of Ti–13Nb–13Zr alloy. Surf Coat Technol 2012;213:239–46.
[8] Qian Y, Jiang M, Zhang Z, Huang Hu, Hong J, Yan J. Microstructures and mechanical properties of Zr-based metallic glass ablated by nanosecond pulsed laser in various gas atmospheres. J Alloy Compd 2022;901:163717.
[9] Qian Y, Jiang M, Zhang Z, Huang Hu, Yan J. Surface functionalization of Zr-based metallic glass by direct nanosecond laser texturing. Vacuum 2021;194:110635.
[10] Gao Q, Ouyang Di, Liu X, Wu S, Huang X, Li N. Fabricating colorful bulk metallic glass surfaces by femtosecond laser processing. Mater Chem Phys 2021;266:124561.
[11] Zhang H, Qian Y, Zhang L, Zhang Di, Liu H, Huang Hu. Surface coloration of Zr-based metallic glass by nanosecond pulsed laser irradiation in ambient atmosphere. Mater Lett 2021;304:130721.

[12] Hong J, Qian Y, Zhang L, Huang Hu, Jiang M, Yan J. Laser nitriding of Zr-based metallic glass: An investigation by orthogonal experiments. Surf Coat Technol 2021;424:127657.
[13] Chan C-W, Lee S, Smith G, Donaghy C. Fibre laser nitriding of titanium and its alloy in open atmosphere for orthopaedic implant applications: Investigations on surface quality, microstructure and tribological properties. Surf Coat Technol 2017;309:628–40.
[14] Huang H, Jiang M, Yan J. The coupling effects of laser thermal shock and surface nitridation on mechanical properties of Zr-based metallic glass. J Alloy Compd 2019;770:864–74.
[15] Do D, Li P. The effect of laser energy input on the microstructure, physical and mechanical properties of Ti-6Al-4V alloys by selective laser melting. Virt Phy Prototy 2016;11(1):41–7.
[16] Phinney L, Rogers J. Pulsed laser repair of adhered surface-micromachined polycrystalline silicon cantilevers. J Ashe Sci Technol 2003;17(4):603–22.
[17] Xu J, Zou P, Wang W, Kang Di. Study on the mechanism of surface topography evolution in melting and transition regimes of laser polishing. Opti Laser Technol 2021;139:106947.
[18] Zhu J, Li L, Li D, Li X, Zhong H, Li S, et al. Microstructural evolution and mechanical properties of laser repaired 12Cr12Mo stainless steel. Mater Sci Eng A 2022;830:142292.
[19] Hafiz A, Bordatchev E, Tutunea-Fatan R. Influence of overlap between the laser beam tracks on surface quality in laser polishing of AISI H13 tool steel. J Manu Process 2012;14(4):425–34.
[20] Xu Z, Ouyang W, Liu Y, Jiao J, Liu Y, Zhang W. Effects of laser polishing on surface morphology and mechanical properties of additive manufactured TiAl components. J Manuf Process 2021;65:51–9.
[21] Cheng K, Xi M, Chen S, Cui G, Zhou H. Microstructures and mechanical properties of Ti6Al4V alloy repaired by the technology of point-mode forging and laser repairing. Opt Laser Technol 2021;144:107410.
[22] Tan C, Zhao L, Chen M, Cheng J, Yang H, Liu Qi, et al. Morphology evolution mechanisms and localized structural modification of repaired sites on fused silica optics processed by CO2 laser rapid ablation mitigation. Opt Laser Technol 2022;147:107648.
[23] Karimi J, Antonov M, Kollo L, Prashanth KG. Role of laser remelting and heat treatment in mechanical and tribological properties of selective laser melted Ti6Al4V alloy. J Alloy Compd 2022;897:163207.